Title

A novel method of surveying submerged landslide ruins: Case study of the Nebukawa landslide in Japan

Shintaro Yamasaki

Kitami Institute of Technology
Corresponding Author, E-mail: yamasaki@mail.kitami-it.ac.jp
Address: Koen-Cho 165, Kitami, Hokkaido, 090-8507, Japan
Phone & Facsimile: +81-157-26-9481

Toshitaka Kamai

Kyoto University, Disaster Prevention Research Institute
E-mail: kamai.toshitaka.3z@kyoto-u.ac.jp
Address: Gokasho, Uji, Kyoto, 611-0011, Japan

Abstract

We investigated submerged ruins from the 1923 Nebukawa landslide, which was caused by the 1923 Kanto earthquake. The on-land areas affected by the landslide have been restored and evidence of the landslide is mostly gone, but huge structures that appear to be man-made have been observed by divers on the seafloor near the area of the landslide. We used a fish finder designed for leisure use and other low-cost equipment to conduct a marine acoustic survey. Because the affected area off Nebukawa is close to shore and shallow and the tools were sufficiently lightweight, we were able to use an inflatable raft for the survey. We created a bathymetric map and side-scan images showing features of the landslide mass and scattered huge structures exposed on the seafloor. After the acoustic investigations, we conducted a diving investigation and were able to ascertain that the structures were made of concrete and were most likely parts of the old Nebukawa station. The ruins were displaced about 260 to 320 m horizontally from the original station location (to 110–170 m offshore) and were mixed with coarse rock fragments from the landslide mass. The distribution of bottom materials suggests that the landslide struck the seafloor and then traveled as far as 460 m offshore from the coastline. The landslide had an equivalent coefficient of friction (H/L) of about 0.15, indicating high mobility. The landslide probably transformed into a turbulent flow mixed with basal sandy sediments, which propelled the debris farther offshore.

Key words

Landslide, Submerged ruins, Acoustic investigation, Fish finder, Side-scan sonar

Highlights

- A submerged landslide and its ruins were investigated with a low-cost fish finder.
- The shape of landslide mass and the bottom materials in the water were obtained.
- The flow processes of a highly mobile submerged landslide were discussed.
- The method is useful for surveying the topography of shallow nearshore waters.

1 Introduction

There are many underwater ruins around the world. The ruins became submerged in a variety of ways, including through long-term sea level changes and the occurrence of geohazards such as floods, tsunamis, tidal waves, and landslides. In earthquake-prone areas such as Japan, historical records document the occurrence of sudden landslides in coastal areas that have swept residences and other infrastructure into the sea or lakes. For example, in the 1792 Unzen Mayuyama landslide, a volume of 3.4×10^8 m^3 swept through Shimabara killing about 10,000 people. The landslide reached the sea and caused tsunamis that killed another 5000 people in and around Ariake Bay (Tsuji and Hino, 1993; Hoshizumi et al., 1999). Recent archaeological investigations have revealed other submerged ruins related to geohazards. For example, off the Nile Delta in Egypt, the submerged ruins of a Greek city have been found, and their submersion was attributed primarily to flooding that occurred in the 8th century AD (Stanley et al., 2001). In 2000s, Hayashi and his research group began to investigate 10th century submerged ruins in Lake Biwa, Japan, by conducting dives and acoustic marine surveys. They inferred that these ruins were carried into the lake by landslides induced by the liquefaction of lakeside sediments (Hayashi et al., 2012). The inundation of the famous submerged ruins of Port Royal, Jamaica, has been attributed to an earthquake that occurred in 1692. The aim of these studies of ancient ruins is not only to conduct archeological research but also to estimate the vulnerability of areas to future hazards, particularly residential coastal areas. In earthquake-prone areas such as Japan, earthquakes frequently induce landslides and tsunamis, and the ruins left behind often provide useful information for dating the events. Underwater ruins are often well preserved after the disaster because they are rarely affected by human activities or long-term weathering. However, few studies have investigated underwater ruins related to geohazards because of the difficulties in surveying such areas.

In this study, we examined submerged ruins related to the 1923 Nebukawa landslide, which was induced by the 1923 Kanto earthquake. The landslide occurred when a steep sea-facing slope collapsed. The landslide went through parts of Nebukawa village, sweeping the Nebukawa train station and trains into the sea and causing 111 deaths. Since the landslide, no underwater scientific investigation has been conducted in this area, and the distribution of the deposits carried by the landslide has not been elucidated. However, some artificial blocky structures have been observed at a depth of 5–10 m on the seafloor by divers in the area. We investigated these structures and the topography in the underwater area affected by the landslide and inferred the landslide movement process. There is currently little information available about submerged landslides.

Marine acoustic technologies have conventionally been employed to investigate underwater ruins, shipwrecks, and seafloor topography (e.g., Hobbs et al., 1994; Singh et al., 2000; Stanley et al., 2004). However, these surveys are usually difficult to conduct and are quite expensive because heavy equipment and large boats must be used. In addition, vessels equipped for scientific research usually cannot operate near the coastline, and they therefore cannot survey areas where the water is less than 10 m deep. Because of these restrictions, we investigated the area in the sea inferred to be affected by the landslide by using a commercially available fish finder designed for leisure use. Some new finders have side-scan sonar systems, and such systems can couple the recorded sounding data with location data obtained by the global navigation satellite system (GNSS). In addition, the fish finder can be operated from an inflatable raft that can be used in shallow waters near the shore. We developed a method employing the fish finder to investigate the ruins and the characteristics and processes of the 1923 Nebukawa landslide. The method was shown to have a strong potential for application in the field of engineering geology, for example, in analyzing coastal erosion as well as monitoring volcanic topography and submarine landslides.

2 The 1923 Nebukawa landslide and its geologic setting

The Nebukawa landslide occurred in Nebukawa, near Odawara, Japan, on 1 September 1923 (Fig. 1). The landslide was one of several induced by the 1923 Kanto earthquake (M 7.9), which was the most catastrophic natural disaster in Japan's history, because it affected the Kanto region (including Tokyo metropolitan region), causing about 100,000 fatalities.

The landslide triggered by the earthquake swept a train that was stopped at the old Nebukawa station into the sea. According to an official report (Ministry of Railways Japan, 1923), the station building (155 m^2), the platform (158 m^2), 11 train cars, and some parts of the track were swept away. Kamai (1991) inferred the affected area from the top of the landslide to the shoreline to be about 60,000 m^2. Other than station buildings, the landslide also carried two wooden houses from the slope above the station into the sea, but their inhabitants managed to escape (Kamai, 1991). In addition, eyewitness Ichimasa Uchida stated that abundant landslide deposits temporarily filled the sea at the shoreline, but they rapidly disappeared as a result of wave action.

This area is below the outer rim of the Hakone Caldera (Fig. 1A). The 1923 Kanto earthquake triggered many landslides on the slopes below the outer rim. After the Nebukawa landslide, another slide moved down along the Shiraito River, south of

Nebukawa, as a debris flow (Fig. 1B). The slope that collapsed during the Nebukawa landslide consisted of andesite, lapilli tuff, and pumice tuff strata of volcanic origin in a slightly inclined sequence (Kuno, 1950; The Geological Society of Japan Geological Leaflet, 2007; Kamai, 1990). Kamai (1990) inferred that the rupture surface was within the pumice tuff layer (Fig. 2). Although this layer inclined only about 10° toward the sea and the layer was only about 1 m thick, its uniaxial strength was extremely low, 3 MPa (in contrast, the strength of the upper andesite lava was 10^4 MPa and the lower lapilli tuff was 10^2 MPa). The pumice tuff layer had been altered by weathering and/or hydrothermally and thus contained abundant clay. This type of layer is easily sheared and can also hold a good deal of moisture. The annual precipitation in this area is more than 2000 mm, which also keeps the moisture level high. Moisture entering the clay-rich material originating from the altered pumice could easily cause it to become fluidized, so under the right conditions the layer of rock above the pumice tuff layer could slide, even with the relatively gentle slope of 10°.

In the 90 years since the landslide, the original topography of the Nebukawa landslide has been lost because of the ensuing recovery activities and land-use changes. However, the topography, landslide mass, and debris in the sea have not been disturbed by human activities. Some large blocky structures exposed on the seafloor have been observed by local divers for years. In 1923, most Japanese houses were made of wood, so if the observed structures are made of concrete, they are most likely remnants of the old Nebukawa station.

3. Marine acoustic investigation

The application of acoustic reflections is a conventional method to obtain data on water depth, underwater topography, and bottom materials. A single-beam echo sounder (or single beam sonar) is used to measure depth and detect objects just beneath a ship; fish finders employed for leisure use are an example. Multi-beam sonars can measure multiple depth data simultaneously and have been used on scientific research vessels, but those systems are expensive and too heavy to be used on small boats, such as the inflatable raft that we used for our survey of shallow nearshore waters. Modern fish finders are small enough to be used on smaller boats. Some newer fish finders also employ GNSS to couple recorded depths with location information. Some leisure-use fish finders employ a side-scan sonar system, which enables them to obtain a wider image of the seafloor. In a side-scan sonar system, the transducer sends two fan-shaped acoustic beams to the seafloor and receives their reflections. The shapes, asperities, and sizes of bottom materials can be recognized by the shading in the sonar images. For example, large boulders or structures make long shadows in the direction opposite the transducer's signal (Fig. 3). Hence, we were able to use relatively unspecialized, inexpensive, and widely available marine technology to study the structures and materials in the study area.

For our investigation, we used a HDS-5 Gen2 fish finder (Lowrance, US), which was capable of obtaining consecutive location information to within 3 m horizontally through the use of a built-in GNSS system. The transducer on the fish finder was a B60 (Airmar Technology Corporation, France) with an assigned frequency of 200 kHz. The minimum recordable depth interval was 1 cm. The data obtained by this transducer were used to create a bathymetric map because the fish finder has a narrower measuring interval than the side-scan sonar. We also used a side-scan sonar system (StructureScan LSS-HD, Lowrance) to record consecutive sonar and side-scan images and depth information on an SD card. The side-scan sonar system had a 25-cm-long transducer with an assigned frequency of 800 kHz. Both systems were powered with a 12-V lead acid battery. The total weight of both systems, including the battery, was about 20 kg, so we were able to place the equipment on a small inflatable raft that could navigate the shallow waters of the study area (Fig. 4).

The bathymetric survey was conducted in shallow water (<30 m) over an area of 800 m × 800 m at intervals of 1 second of latitude. The side-scan survey was conducted over a smaller part of this area (500 m × 600 m) along 14 measurement lines. Side-scan images were captured directly from the display of the fish finder.

We extracted consecutive location information with coordinates and depths with DrDepth 5.0 software (PerPelin, Sweden), a sea-bottom mapping software application, from the data obtained by the fish finder. We then corrected for changes in tide. We used the mapping software Surfer 11 (Golden Software, US) to construct a contoured bathymetric map. Interpolation was done by the kriging method. Then, to generate a geometrically corrected map, we corrected the coordinates of point data with Japanese rectangular plain system VIII, for which the origin point is E138°30'00", N36°00'00".

Follow-up diving investigations were conducted after the acoustic investigations to confirm the findings of the acoustic survey and to determine the types of materials in the large structures.

4 Results

4.1 Topography and bottom materials

The bathymetric map we created is shown in Fig. 5. Small mounds, indicated by closed contour lines, are situated in the water at depths of 6 m to 24 m offshore of the beach area buried by the 1923 Nebukawa landslide. The slope immediately offshore of the landslide area and the mouth of Shiraito River is relatively more gentle than it is farther offshore in the mapped area.

A synthetic side-scan image is shown in Fig. 6A. The bottom materials can be divided into two main types: rudaceous (large rock fragments) and arenaceous (sand-sized fragments). A rudaceous area spreads along the shoreline and extends tongue-like about 460 m offshore; its shape is irregular in the southern part of the mapped area. Three isolated rudaceous areas are also distributed offshore of the mouth of the Shiraito River.

The raw side-scan images show the composition of the bottom materials in more detail (Fig. 6B). The density of observable sized rocks (larger than several dozen centimeters) decreases with distance from the shore, but the boundary between rudaceous and arenaceous areas is clear. Although there is some image skew, some angular rocks appear in the rudaceous area. There are also some huge bodies (larger than several meters) in the deeper arenaceous areas (Fig. 6B, C–C′).

4.2 Submerged ruins

The side-scan images suggest the presence of at least 10 prominent polygonal bodies at depths of 6 to 10 m on the rudaceous bottom (Fig. 7). These structures have been observed by divers and have been speculated to be submerged ruins from the landslide. These ruins can be divided into four groups by their distribution: group I consists of four angular bodies with maximum lengths of about 3, 10, 10, and 10 m; group II consists of three angular bodies, about 6, 8, and 11 m long; group III consists of one angular body about 5 m long; and group IV consists of two angular bodies, with lengths of 5 and 11 m.

After the acoustic survey, we conducted a diving investigation near groups I and II, and confirmed that the largest angular structure was made of concrete (Fig. 8A). We also observed a steel bar resembling a rail near group II (Fig. 8B). The ruins of groups III and IV were similar in shape and size to the large bodies in groups I and II. The ruins are directly situated on angular rock fragments that had no rounding ablation (Fig. 8B).

5 Discussions

The topography and bottom materials observed in our study area show common characteristics of a landslide. The presence of the ruins is also consistent with a landslide in the area. The slope of the seafloor offshore of the area near the Nebukawa landslide is gentle. We infer that the mounds observed in this area were formed by the landslide because such mounds are often observed in areas where landslides have occurred. The ruins are situated on angular rock fragments (Fig. 8B) that lack rounding ablation; such fragments are usually made by mechanical fracturing during a landslide. The side-scan imaging showed angular rock fragments in the deeper parts of the rudaceous areas (Fig. 6B). Thus, the rudaceous areas were created by the landslide.

The size and shape of the Nebukawa landslide can be estimated from the bottom material data (Figs. 5 and 6). The rudaceous areas in Fig. 6 were made by the landslide, whereas the arenaceous areas were undisturbed by the landslide. The original arenaceous bottom was affected by sediment discharged from the Shiraito River before the 1923 Kanto earthquake. Sediment discharged from the river intensively affects the southern part of the rudaceous area, which has an irregular shape. In addition, when the 1923 Kanto earthquake occurred, debris also flowed from the river into the sea and covered the southern part of the Nebukawa landslide (i.e., the near-shore rudaceous area). The Nebukawa landslide may have spread farther south, but we could not confirm that using our methods. The distribution of the bottom materials indicates that the landslide mass traveled at least 460 m from the coast. Thus, the maximum horizontal distance of the landslide was at least 840 m and the vertical drop was 125 m (Figs. 2 and 5), indicating that the equivalent coefficient of friction (H/L) was about 0.15 (the apparent friction angle is 8.5°). This value is quite small, but it is close to that of other submarine landslides (Masson et al., 2006).

The location of ruins in the landslide mass provides information about the landslide processes. The ruins are located in the sea at a horizontal distance of about 260 to 320 m from the old Nebukawa station, or about 110 to 170 m from the coast. The calculated total area of the ruins obtained from the side-scan images is 220 m^2 , which is reasonably close to the estimated total size of the station and platform (313 m^2; Ministry of Railways Japan, 1923). Other ruins may have been deposited just after the event, but we did not find ruins in water shallower than 6 m. If they were deposited in these shallow areas, they probably have been removed by wave erosion or human activity. The ruins consist of broken fragments scattered on the seafloor, and it was difficult to positively identify them as parts of a station platform. However, the large fragments are clustered in an area from about 70 m to about 170 m offshore. This placement is consistent with the findings of Kamai (1990), who inferred that the landslide was relatively cohesive. The landslide mass, however, extends offshore about 460 m beyond the ruins. Because the old Nebukawa station was located on the lower part of the slope where the landslide occurred, most of the materials in the landslide originated upslope of the station. If the station and platform were moved directly from their original position to the present position of the ruins, the collapsed area, which was downslope of the station and about 50–100 m long, was likely to spread out over 300 m long. The landslide probably transformed into a turbulent flow mixed with basal sandy sediments, which enabled the landscape debris to travel farther offshore. Sand-rich flows sometimes travel longer distances in water with turbulence as a hyperconcentrated flood flow as compared to the flow of debris that is rich in gravel-sized rocks (Sohn et al., 2002). In addition, basal sandy sediment with a high pore-water pressure may reduce basal friction, which could also increase the distance traveled. There are some huge bodies outside of the rudaceous area (Figs. 5 and 6B); they may also have been transported via turbulent flow.

6 Conclusions

We used a simple and low-cost method to clarify the topography and geologic characteristics of the 1923 Nebukawa landslide and the submerged ruins carried by the landslide into the sea. The side-scan imaging revealed landslide materials as far as 460 m from the coast, making the total length traveled 840 m and suggesting that the landslide was highly mobile, with an equivalent coefficient of friction (H/L) of about 0.15. The landslide mass was transformed into a turbulent flow mixed with basal sandy sediments, which greatly expanded the affected area. The results showed that this submerged landslide probably expanded over a wider area than we originally expected, a possibility that would be important to take into account for hazard mitigation in shallow water areas. The submerged ruins observed in this study are both a valuable memorial and an educational resource that can help us to better understand the details of the 1923 Kanto earthquake.

Our marine investigation method using a fish finder and an inflatable raft proved useful for surveying in shallow and other areas close to the shore. The method is low cost and mobile and allows researchers to study narrow and shallow areas that other scientific research vessels cannot reach. Side-scan sonar imaging is a powerful technology that can be used to identify bottom materials, but we were unable to obtain depositional fabrics that indicate flow directions or flow units because of image skew, in particular images that were stretched as a result of the vessel changing speed. We currently do not have a solution for this difficulty, but solving this challenge would allow researchers to obtain information to better understand landslide processes. Comparing images obtained from various scanning directions and doing a composite analysis could be one way to obtain data for a flow direction analysis.

Acknowledgements

We developed the equipment for the marine investigation with the assistance of the Technical Division and Engineering Center and the Kussharo Lake Training Institute of the Kitami Institute of Technology, and the Toya Lakeside Training Institute of Hokkaido University. Masahiro Hiramatsu of the Kitami Institute of Technology was particularly helpful. NHK (Japan Broadcasting Corporation) and the NHK Special "MEGAQUAKE" group of reporters also helped with our on-site investigation. This work was supported by a Grant-in-Aid for Scientific Research (Grant No. 23710206 to S.Y. and No. 26560187 to S.Y). We thank all of those who helped with the research.

References

The Geological Society of Japan Geological Leaflet eds., 2007. 1. Hakone Volcano. The Geological Society of Japan (in Japanese).

Hayashi, H., Kamai, T., Haraguchi, T., 2012. Submerged Villages in Lake Biwa (Jishin-de-shizunda-kotei-no-mura). ISBN: 978-4-88325-468-2, pp.137 (in Japanese).

Hobbs III, C.H., Blanton, D.B., Gammisch, R.A., Broadwater, J., 1994. A Marine Archaeological Reconnaissance Using Side-Scan Sonar, Jamestown Island, Virginia, USA. Journal of Coastal Research, 351-359.

Hoshizumi, H., Uto, K., Watanabe, K., 1999. Geology and eruptive history of Unzen volcano, Shimabara peninsula, Kyushu, SW Japan. Journal of Volcanology and Geothermal Research 89, 81-94.

Kamai, T., 1990. Failure mechanism of deep-seated landslides caused by the 1923 Kanto earthquake, Japan, Proceedings of the Sixth International Conference and Field Workshop on Landslides, pp. 187-198.

Kamai, T., 1991. Failure Mechanism of Landslide with "squeezing-out" deformation--1923 Nebukawa-station Landslide, Journal of Japan Landslide Society 27, 1-8. (In Japanese with English Abstract)

Kuno, H., 1950. Petrology of Hakone volcano and the adjacent areas, Japan. Geological Society of America Bulletin 61, 957-1020.

Masson, D., Harbitz, C., Wynn, R., Pedersen, G., Løvholt, F., 2006. Submarine landslides: processes, triggers and hazard prediction. Philosophical Transactions of the Royal Society A: Mathematical, Physical and Engineering Sciences 364, 2009-2039.

Ministry of Railways Japan, 1923. The report of the railway damage investigation of the 1923 Kanto earthquake (Taisho-12-nen-tetsudo-shingai-cho-sasho). The Ministry of Railways Japan, pp.147 (in Japanese).

Singh, H., Adams, J., Mindell, D., Foley, B., 2000. Imaging underwater for archaeology. Journal of Field Archaeology 27, 319-328.

Sohn, Y.K., Choe, M., Jo, H., 2002. Transition from debris flow to hyperconcentrated flow in a submarine channel (the Cretaceous Cerro Toro Formation, southern Chile). Terra Nova 14, 405-415.

Stanley, J.-D., Goddio, F., Schnepp, G., 2001. Nile flooding sank two ancient cities. Nature 412, 293-294.

Stanley, J.-D., Goddio, F., Jorstad, T.F., Schnepp, G., 2004. Submergence of ancient Greek cities off Egypt's Nile Delta-A cautionary tale. GSA today 14, 4-10.

Tsuji, Y., Hino T., 1993. Damage and Inundation Height of the 1792 Shimabara Landslide Tsunami along the Coast of Kumamoto Prefecture. Bulletin of the Earthquake Research

Institute, University of Tokyo 68, 91-176. (In Japanese with English abstract)

Figures

Fig. 1

(A) Index map of the 1923 Nebukawa landslide and the 1923 Kanto earthquake. (B and C) Areas affected by the landslide and the 1923 Ohbora debris flows from the Shiraito River (based on the estimates of Kamai, 1990). The geologic profile of the line L–L' is shown in Fig. 2.

Fig. 2

Vertical cross section along line L–L' showing the geology of the Nebukawa area. The onshore geology is based on Kamai (1990), and the offshore geology is based on this survey.

Fig. 3

Basic concept of side-scan sonar surveying and sonar images. Further details are discussed in the text.

Fig. 4

(A) Schematic diagram of the fish-finder system and (B) photo of the inflatable raft equipped with the transducers. Further details are discussed in the text.

Fig. 5

(A) Topographic and bathymetric map of the area shown in Fig. 1B (contour interval on land and under water, 2 m). The bold black line indicates the boundary of the side-scan sonar scanning area (Fig. 6A). The bathymetric map was generated from data obtained from this study. The topography on land was obtained from 5-m DEM data of the Geological Survey Institute of Japan.

Fig. 6

(A) Synthetic side-scan sonar images indicated in Fig. 5 and (B) selected raw side-scan images from offshore of Nebukawa. The Roman numbers refer to the groups shown in Fig. 7.

Fig. 7

Distribution map of large concrete structures (gray polygons) and a steel bar (rail). The groups, indicated by the Roman numerals, are described in the text.

Fig. 8

Underwater photographs of a concrete structure in group II, and of a nearby steel bar.

Fig.1

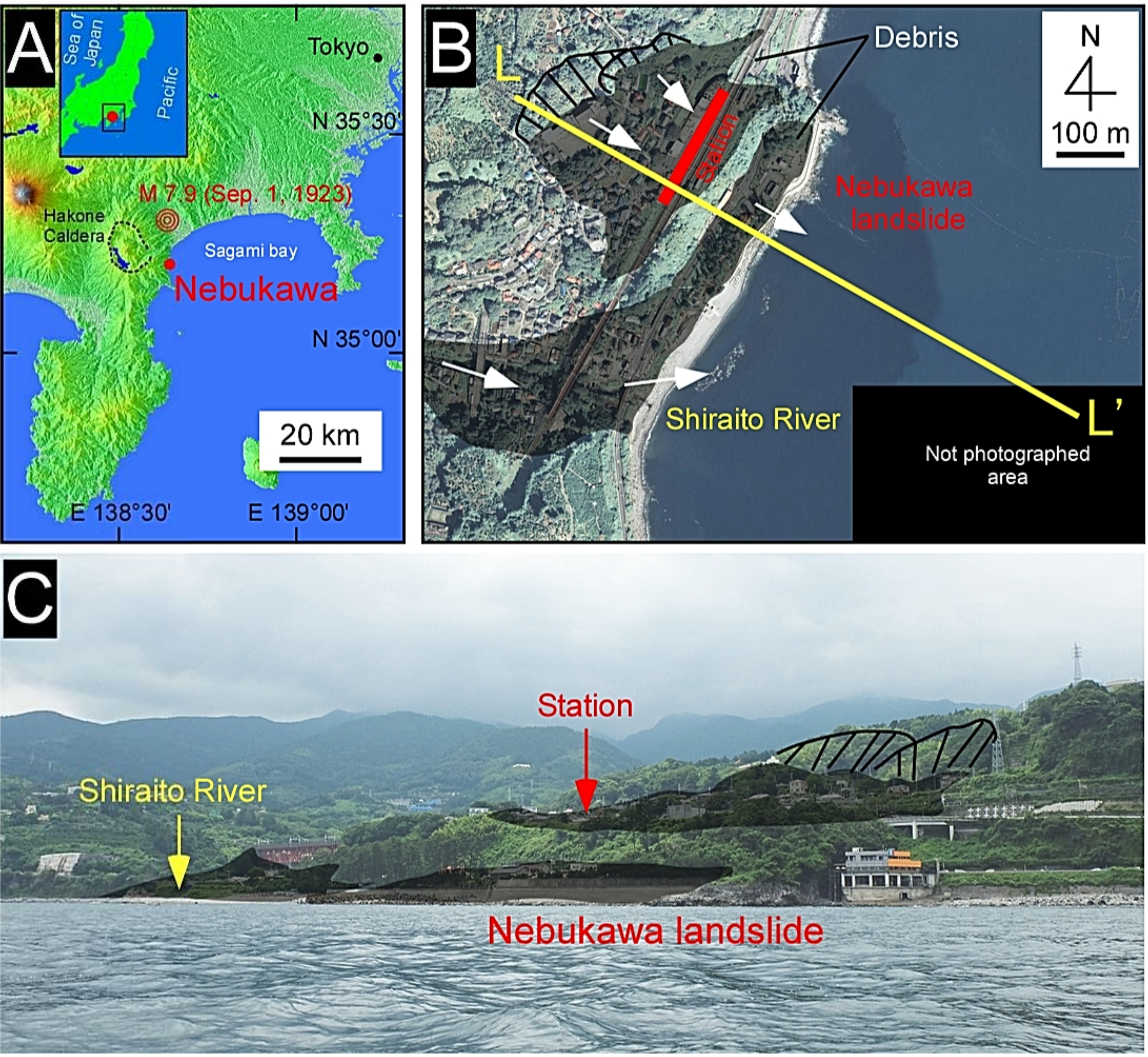
A
Sea of Japan
Pacific
Tokyo
N 35°30'
M 7.9 (Sep. 1, 1923)
Hakone Caldera
Sagami bay
Nebukawa
N 35°00'
20 km
E 138°30'
E 139°00'
B
L
Debris
N
100 m
Station
Nebukawa landslide
Shiraito River
L'
Not photographed area
C
Station
Shiraito River
Nebukawa landslide

Fig.2

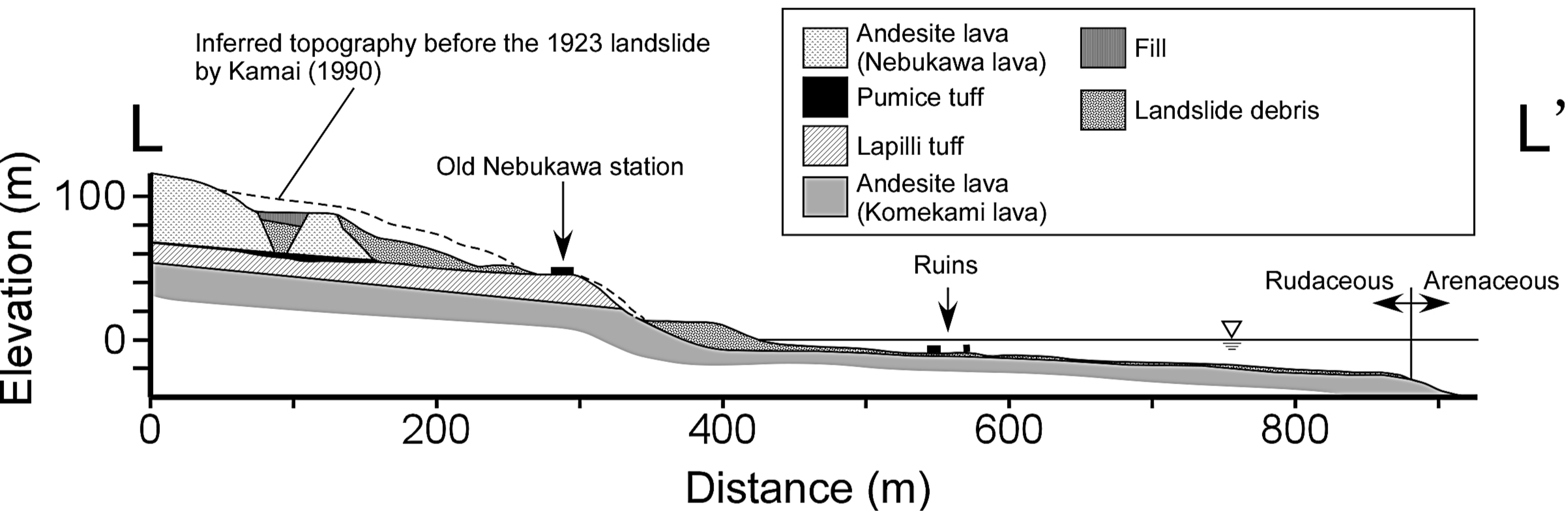
L
L’
Inferred topography before the 1923 landslide
by Kamai (1990)
Old Nebukawa station
Ruins
Rudaceous
Arenaceous
Andesite lava
(Nebukawa lava)
Pumice tuff
Lapilli tuff
Andesite lava
(Komekami lava)
Fill
Landslide debris
Elevation (m)
100
0
0
200
400
600
800
Distance (m)

Fig.3

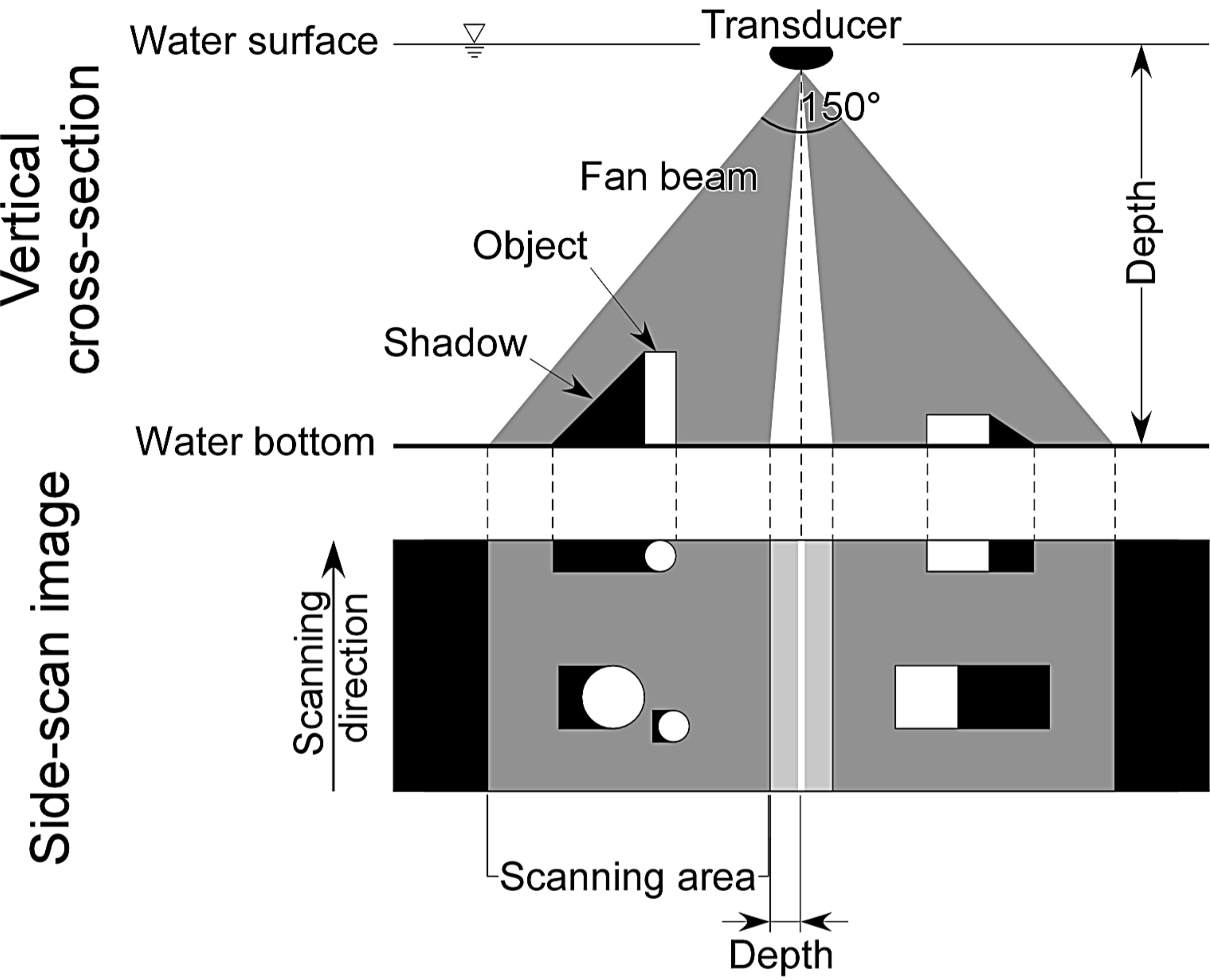

Water surface
Transducer
150°
Fan beam
Object
Shadow
Water bottom
Depth
Vertical cross-section
Side-scan image
Scanning direction
Scanning area
Depth

Fig.4

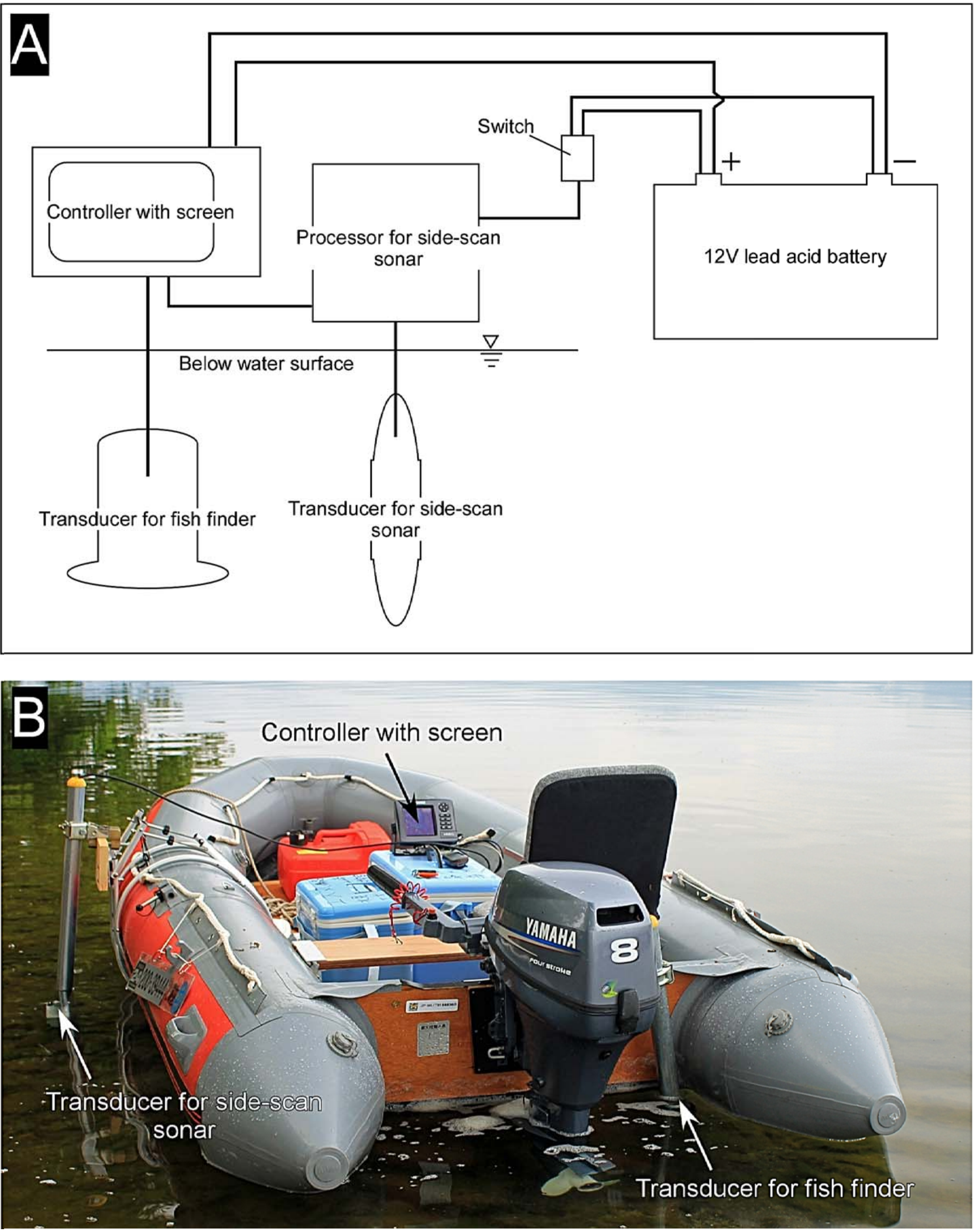
A
Switch
+
−
Controller with screen
Processor for side-scan sonar
12V lead acid battery
Below water surface
Transducer for fish finder
Transducer for side-scan sonar
B
Controller with screen
YAMAHA
8
FOUR STROKE
Transducer for side-scan sonar
Transducer for fish finder

Fig.5

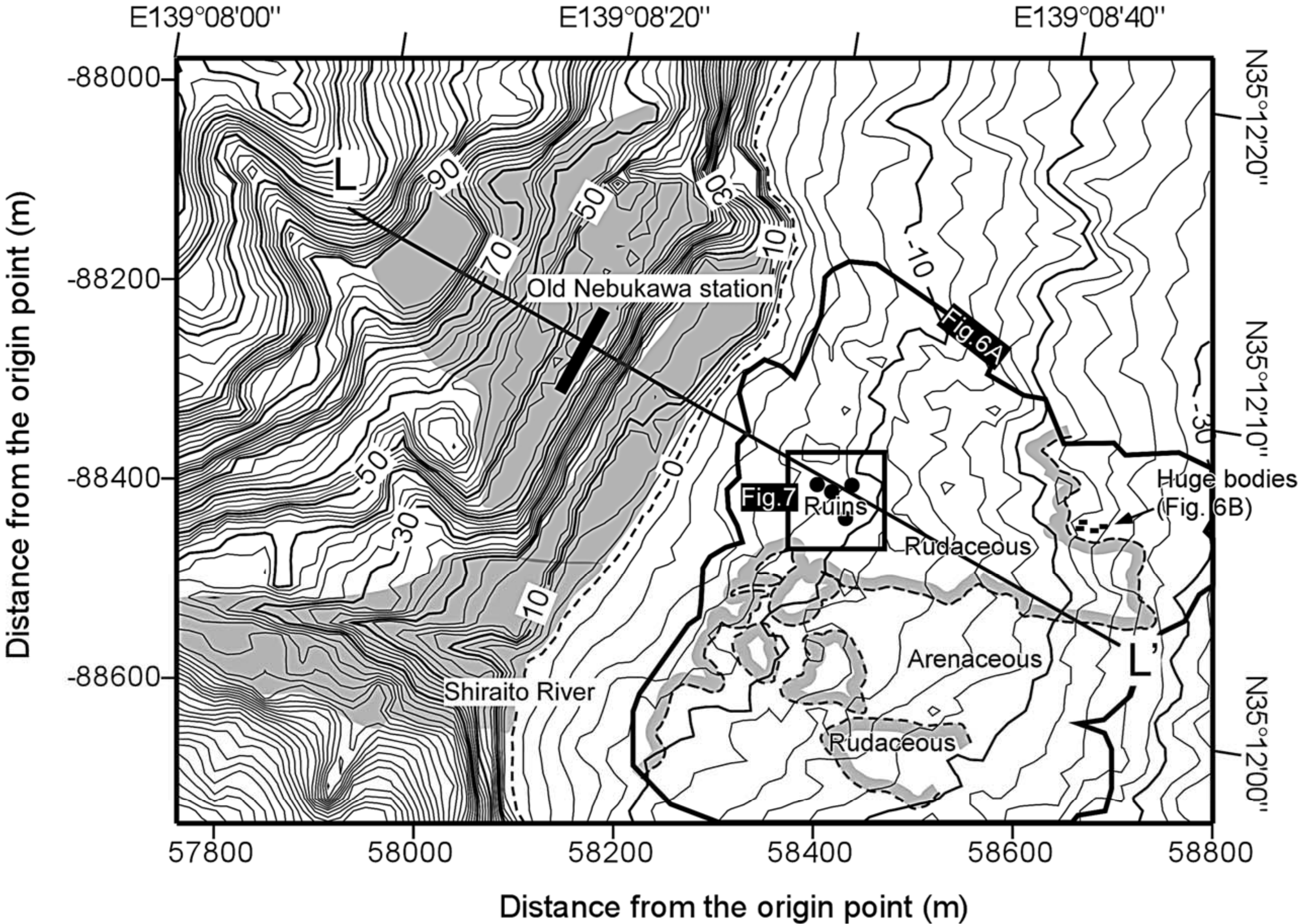
E139°08'00''
E139°08'20''
E139°08'40''
N35°12'20''
N35°12'10''
N35°12'00''
-88000
-88200
-88400
-88600
57800
58000
58200
58400
58600
58800
Distance from the origin point (m)
Distance from the origin point (m)
L
L'
90
70
50
30
10
0
-10
-30
Old Nebukawa station
Shiraito River
Fig.6A
Fig.7
Ruins
Rudaceous
Arenaceous
Rudaceous
Huge bodies
(Fig. 6B)

Fig.6

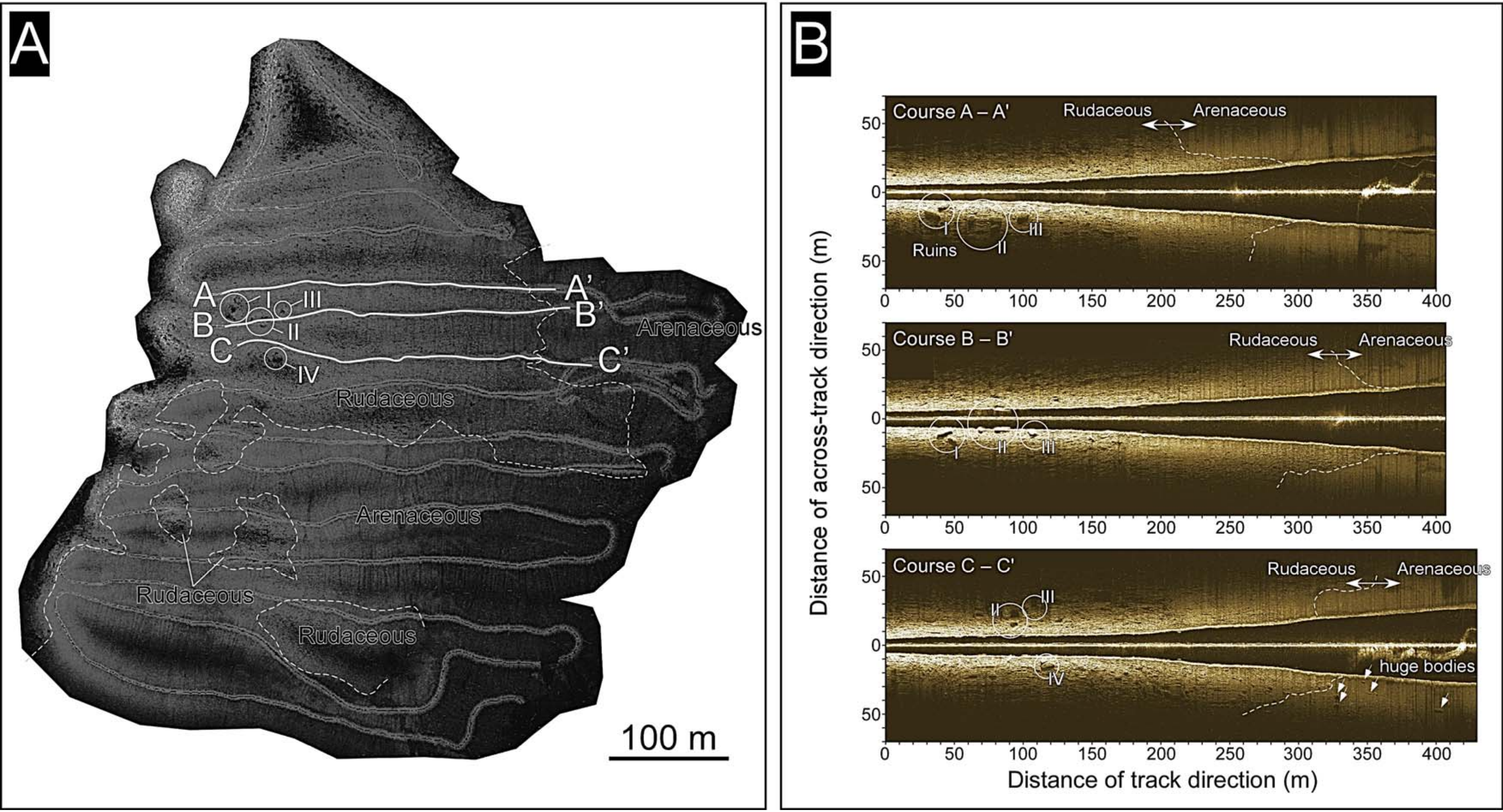

A
A
A'
B
B'
C
C'
I
II
III
IV
Rudaceous
Arenaceous
Arenaceous
Rudaceous
Rudaceous
Arenaceous
100 m
B
Course A – A'
Rudaceous
Arenaceous
Ruins
Course B – B'
Course C – C'
huge bodies
Distance of across-track direction (m)
Distance of track direction (m)
0
50
100
150
200
250
300
350
400

Fig. 7

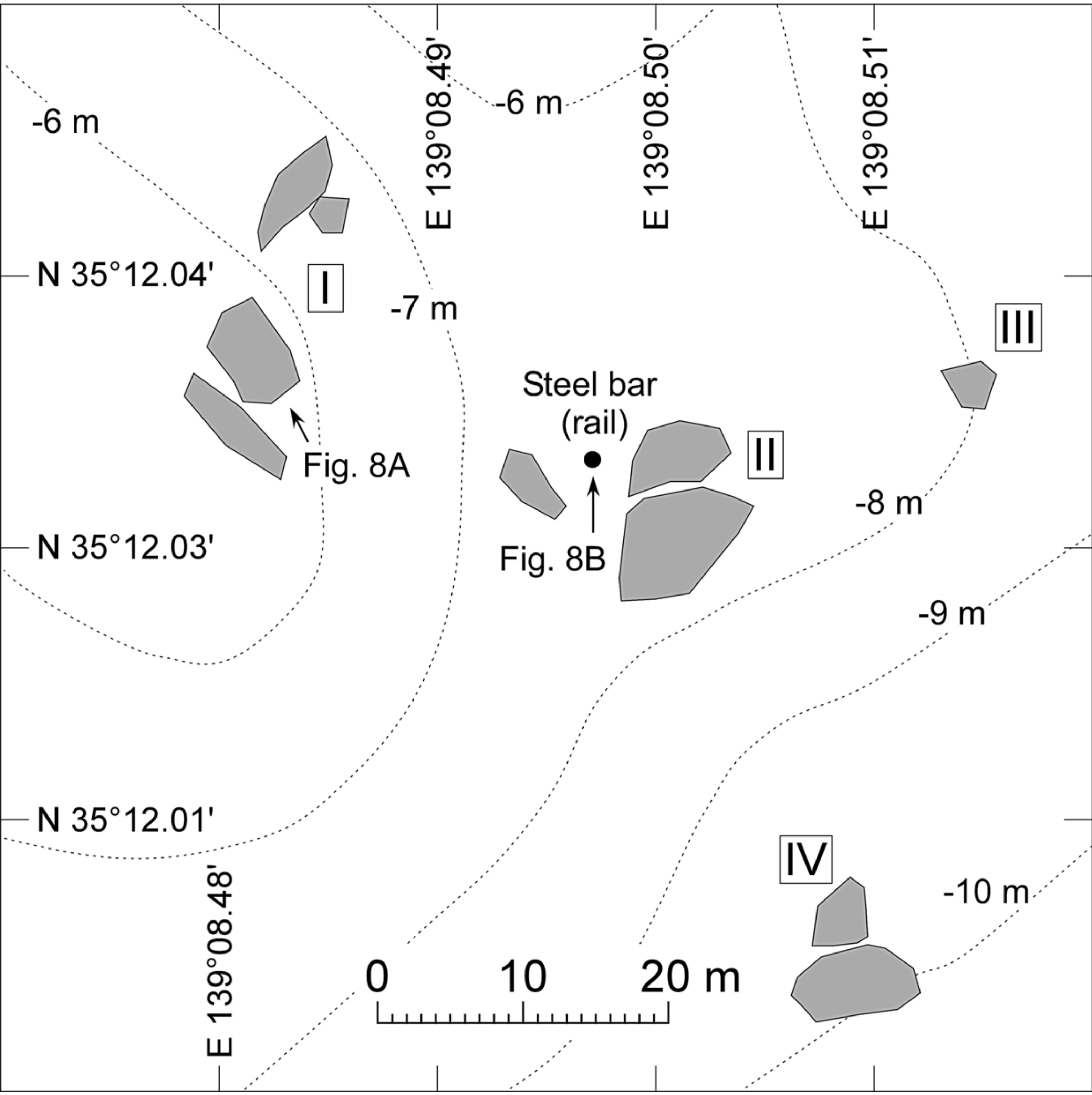
E 139°08.49'
E 139°08.50'
E 139°08.51'
E 139°08.48'
N 35°12.04'
N 35°12.03'
N 35°12.01'
-6 m
-6 m
-7 m
-8 m
-9 m
-10 m
I
II
III
IV
Steel bar
(rail)
Fig. 8A
Fig. 8B
0
10
20 m

Fig.8

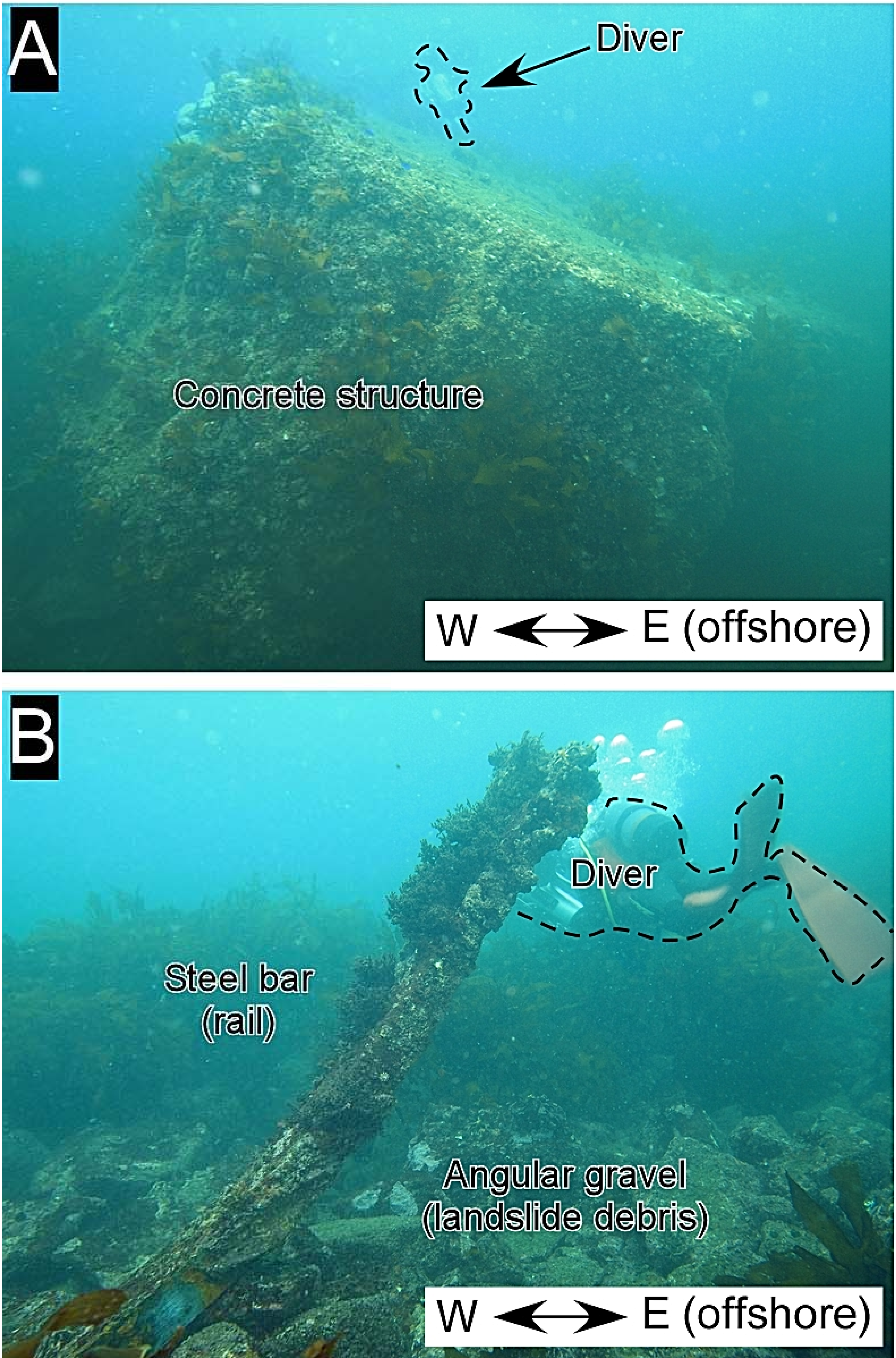
A
Diver
Concrete structure
W E (offshore)
B
Diver
Steel bar
(rail)
Angular gravel
(landslide debris)
W E (offshore)